ELSEVIER

Journal of Power Sources 114 (2003) 277–284

JOURNAL OF POWER SOURCES

www.elsevier.com/locate/jpowsour

A sealed optical cell for the study of lithium-electrode|electrolyte interfaces

P.C. Howlett[a,*], D.R. MacFarlane[a], A.F. Hollenkamp[b]

[a]*Monash University School of Chemistry, Clayton South, Vic. 3168, Australia*
[b]*CSIRO Energy Technology, Bayview Avenue, Clayton South, Vic. 3169, Australia*

Received 25 July 2002; accepted 25 October 2002

Abstract

A sealed, symmetrical, lithium optical cell, which enables optical images of lithium surface deposits and in situ Raman spectra to be obtained simply and conveniently during charge–discharge cycling of lithium metal electrodes, has been designed and tested. A conventional aprotic liquid, 1 M lithium hexafluorophosphate in propylene carbonate, and an experimental ionic liquid, 20 mol% lithium bis(trifluoromethanesulfonyl)amide in 1-ethyl 3-methyl imidazolium bis(trifluoromethanesulfonyl)amide, are investigated as electrolyte solutions. Images obtained from the cell with the former electrolyte solution demonstrate the problems associated with cycling lithium metal electrodes. Images obtained with the latter electrolyte solution provide clear evidence that continued investigation of ionic liquids for use with lithium metal electrodes is warranted. Operation of the cell with the conventional electrolyte yields Raman spectra of good quality. The spectra display vibrational modes which arise from the electrolyte, as well as several additional modes which are associated with the deposits formed during cycling.
© 2002 Elsevier Science B.V. All rights reserved.

Keywords: Battery; Optical images; Raman spectra; Lithium metal electrode; Ionic liquids; Dendrites

1. Introduction

The lithium metal electrode is of great interest to battery researchers and technologists because of its high theoretical specific capacity. To date, however, problems associated with the reversibility of the deposition–dissolution process at the interface have prevented its successful application in secondary batteries for commercial purposes. The poor reversibility is due to non-uniform current density across the lithium surface under an applied potential. This limitation has been related to the formation of an inhomogeneous film on the metal surface. The film, known as the solid electrolyte interphase (SEI), is composed of various reduction products which result from reaction between lithium and the electrolyte solution [1].

Charge–discharge cycling of the electrode requires the transport of lithium ions through the film for the charge-transfer reaction (i.e. $Li^0 \Leftrightarrow Li^+ + e^-$) to occur. The inhomogeneity of the film gives rise to conduction pathways of differing lithium-ion conductivity which, in turn, cause preferential deposition (charging) or dissolution (discharging) at a relatively small number of sites. This feature results in uneven deposition and dissolution at the electrode surface. In batteries that employ conventional aprotic electrolytes—typically, a solution of lithium salts ($LiPF_6$, $LiBF_4$, $LiAsF_6$) in a cyclic carbonate ester solvent—the deposition process causes the formation of acicular crystals of lithium, i.e. 'dendrites' [2]. The resulting electrode has a high surface area and this introduces risks of short-circuits (dendrites can connect electrodes of opposite polarity), irreversible loss of capacity through detachment of deposits from the substrate (dead lithium), and the development of electrolyte reduction products which passivate the newly formed surface. In the event of a short-circuit, current passing through a thin dendritic 'connection' will rapidly generate heat and, consequently, introduce the safety hazards of fire and explosion.

Researchers have employed a wide range of techniques to study the processes which occur on the lithium surface during cycling, especially in the presence conventional polar aprotic electrolyte systems [3–12]. Polymer electrolyte|lithium interfaces have also been the subject of intense study [13–15]. Numerous investigations have employed 'optical cells' to study interfacial electrode processes, particularly for the lithium-electrode|electrolyte system [16–26]. The studies have focused primarily on elucidation of the

* Corresponding author. Tel.: +61-3-9545-8500; fax: +61-3-9562-8919.
E-mail address: patrick.howlett@csiro.au (P.C. Howlett).

0378-7753/02/$ – see front matter © 2002 Elsevier Science B.V. All rights reserved.
PII: S0378-7753(02)00603-1

mechanism of dendrite formation and on the efficacy of various methods to suppress this phenomenon.

Ionic compounds that are liquid at room temperature, so-called 'ionic liquids', are receiving a great deal of attention as new environmentally benign solvents for a variety of processes, primarily as replacements for conventional media in chemical processes. This is because ionic liquids possess a number of desirable features, namely:

(i) a wide liquid range (room temperature to above 300 °C);
(ii) outstandingly good solvent properties, i.e. an ability to dissolve a wide range of organic and inorganic compounds to high concentration;
(iii) advantages with respect to catalyst recovery and product separation;
(iv) negligible vapour pressure, and hence minimal harmful effects of solvent evaporation on human health and the environment;
(v) re-usable, relatively cheap, and easy to prepare.

Ultimately, the use of ionic liquids could provide 'greener' processes with less waste per unit yield [27,28].

There has also been some interest in the application of ionic liquids as alternative electrolyte solvents for use in alkali metal batteries. Ionic liquids have a wide electrochemical window, high conductivity, high thermal stability, low safety hazards (non-flammable, non-volatile), and low toxicity. Moreover, due to their inert properties, ionic liquids are re-usable [29–34]. The range of available anions and cations which form room temperature ionic liquids has expanded rapidly. It has been estimated that there are approximately one trillion (10^{18}) candidates [28]! Given the combination of advantageous properties and design flexibility (i.e. solvent properties can be adjusted by varying anion–cation combinations), ionic liquids offer a possible solution to the problems that arise at the lithium-electrode|electrolyte interface.

In the work reported here, an optical cell has been constructed to investigate alternative electrolyte systems for use with lithium metal electrodes. The design allows cells to be assembled with very reproducible geometry. It is also necessary for the exposed electrode surface to be very small in order to avoid depth-of-field problems and to approach a situation where the deposits can be viewed as being almost two-dimensional. The latter assists the comparison of images with image-processing software. The cell configuration (i.e. thin, widely separated electrodes) is intended to create a situation where the electrode surface is a representative sub-section of the surface of a battery electrode. Moreover, sealed cells allow observation of the evolution and the build up of gas. This is important given that gas pressure within the cell may influence deposit morphology.

2. Experimental

2.1. Materials

Lithium foil (Aldrich 99.9%) of thickness 180 μm was used as received. Propylene carbonate (PC, Aldrich) was distilled over sodium. Lithium hexafluorophosphate ($LiPF_6$, Aldrich 99.99%) and lithium bis(trifluoromethanesulfonyl)amide (LiTFSA, donated by 3M Company) were dried under vacuum at 70 °C for 48 h. 1-Ethyl 3-methyl imidazolium (EMIm) was synthesised by reacting methylimidazole (Aldrich) with an ethyl halide (Aldrich) to form methylethylimidazolium halide, which was then reacted (metathesised) with LiTFSA to form 1-ethyl 3-methyl imidazolium bis(trifluoromethanesulfonyl)amide (EMImTFSA) and lithium halide (see Fig. 1) [35]. The resulting two products were separated by liquid–liquid extraction. The EMImTFSA was treated in a glovebox with successive additions of freshly cut lithium metal until the lithium surface remained shiny for a period of several days. Surlyn® (DuPont) was used as an adhesive sealant to bind the cell components together, Surlyn® is a transparent thermoplastic resin with good chemical resistance properties. Copper shim (Precision Brand; thickness: 0.025 mm) was used as a current-collector. All cell materials were washed successively in water, acetone and hexane prior to drying under vacuum (50 °C) for 24 h. All materials were stored under a dry argon atmosphere in a glovebox.

2.2. Cell construction

Construction of the optical cell was performed under dry argon in a glovebox. A small piece of lithium foil was rolled into a polished stainless-steel depression to yield a foil with a uniform thickness of 100 μm (4 mm wide × 40 mm long). The resulting foil electrode was washed in hexane, placed in

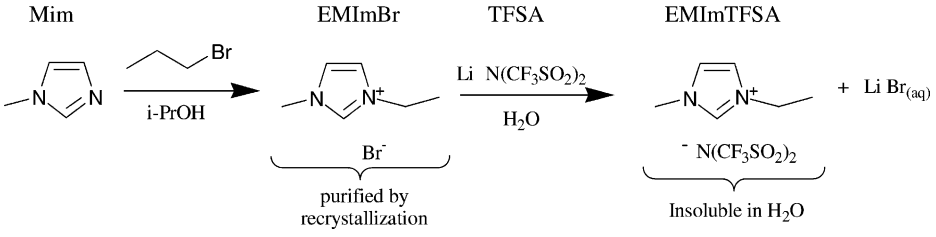

Fig. 1. Synthesis of ethyl methyl imidazolium bis(trifluorosulfonyl)amide.

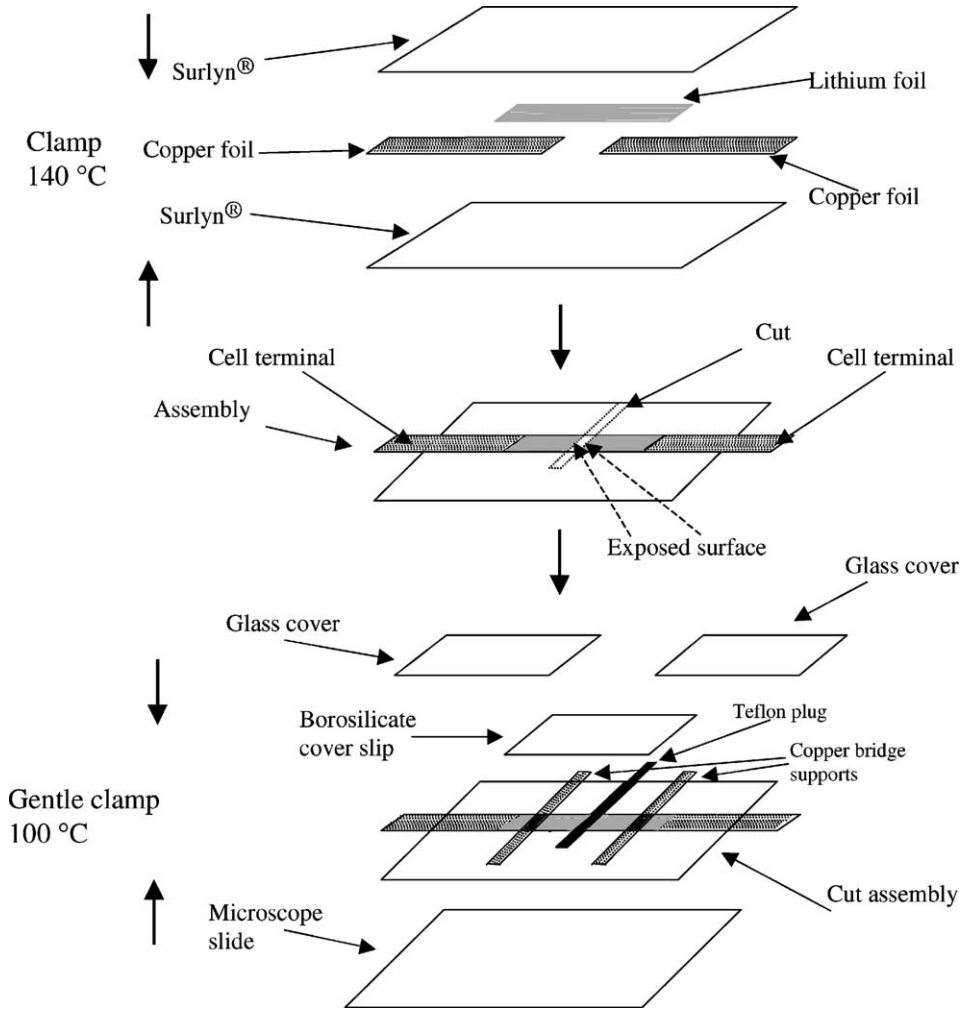

Fig. 2. Schematic representation of assembly of optical cell.

contact with two pieces of copper foil of similar dimensions, and then pressed in a Teflon-lined press to form a single strip of metal (see Fig. 2). The strip was sandwiched between two pieces of Surlyn® (~70 mm × 25 mm), placed in a Teflon-lined clamp, and heated at 140 °C for 30 min. After cooling, a strip of 2 mm width was cut at the centre of the lithium foil to create two exposed lithium surfaces (each 0.004 cm^2 in area) that were separated by a cavity. The assembly was placed on a glass microscope slide and a piece of Teflon (of appropriate dimensions) was inserted between the electrodes with a snug fit. The Teflon effectively plugged the cavity and prevented the Surlyn® from flowing over the electrode surface during the subsequent heating step. Two pieces of copper shim were positioned adjacent to the electrode to form a bridge support. A borosilicate cover-slip was placed on the support. The assembly was returned to the Teflon-lined clamp and (under gentle pressure) heated to 100 °C for ~15 min. Two more pieces of Surlyn® and glass were added, to reinforce the structural integrity of the cell, and the assembly was returned to the clamp at 100 °C for 15 min (see Fig. 2). After cooling, the Teflon plug was removed carefully and the cavity was filled with electrolyte solution by means of a syringe. The cavity was plugged by heating a small piece of Surlyn® with a soldering iron. The sealed cell could then be removed from the glovebox for study.

2.3. Cell cycling

A schematic of the experimental set-up is shown in Fig. 3. Galvanostatic charge–discharge cycling was performed using a CSIRO Battery Controller Unit (BCU) and a programmable microprocessor that logs data to a personal computer. The BCU was interfaced to an EG&G PAR 362 scanning potentiostat. Each cycle consisted of 1 C cm^{-2} of charge passed, at 1 mA cm^{-2}, for each deposition (charge) and dissolution (discharge) step.

The cells were placed on an X–Y–Z stage which was mounted on a marble block on an anti-vibration bench. A personal computer ran National Instruments IMAQ driver software and a PCI-IMAQ-1408 image acquisition card to acquire digital images of the electrode surface from a Pulnix TM-6CN CCD camera that was fitted with a Navitar

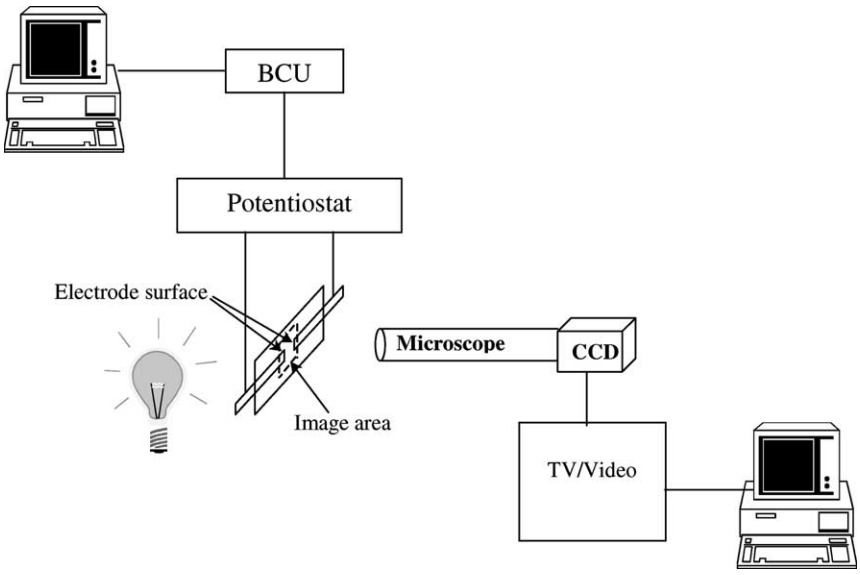

Fig. 3. Schematic representation of equipment used to study electrode processes in optical cell.

1× adaptor lens. The experiments were also recorded on videotape.

3. Results and discussion

3.1. Propylene carbonate–$FiPF_6$ cell

A solution of 1 M $LiPF_6$ in propylene carbonate was used in the development of the cell. Although not commercially viable, this electrolyte is considered to be an appropriate system for comparison with ionic liquids. The evolution of surface deposits in a symmetrical lithium cell under galvanostatic cycling is shown in Fig. 4. On the first deposition cycle, there are immediate observable changes on the electrode surface. With subsequent cycling, both electrode surfaces become almost uniformly covered with voluminous deposits. The deposition and growth of the deposits occur from the base, i.e. close to the electrode surface, rather than from the surface of the deposits. As the deposits advance further into the cell, the outermost deposits do not change in appearance. In some cases, it has been possible to follow the progress of individual, distinctly shaped deposits (such as those indicated within the circle in Fig. 4) for several hundred cycles. There are no significant changes in the morphology of these deposits. Thus, it appears that the deposits are no longer taking part in the charge–discharge process and are most likely examples of 'dead lithium'. Occasionally, rapid motions occur within the mass of the deposit. These are probably the result of deposits pushing against one another and are an indication of the presence of forces that are sufficient for the deposits to pierce a separator and lead to short-circuiting of a cell. It is not difficult to envisage similar behaviour at the surface of a battery electrode under stack pressure. All of the above observations support the published findings of other investigations of the processes of dendrite growth and formation of dead lithium [36–39].

Examination of the voltage profile during cycling also indicates that dendritic growth and the formation of dead lithium have a marked effect on the conductance of the cell (Fig. 5). Initially, the potential required to pass the constant current (1 mA cm^{-2}) is low and stable. After several hundred cycles, the cell begins to fill with deposit and the potential required to maintain the current increases substantially. This indicates an increase in resistance to the transport of lithium ions, possibly due to the presence of a physical barrier of 'dead lithium'. It is likely that this situation would precede to a short-circuit. Heat, generated as a result of the increased resistance, causes softening of the separator. The presence of deposits of 'dead lithium' close to the surface may effectively reduce the active surface area of the electrode and therefore lead to an increase in current density. An increase in deposition current density has been shown to promote dendritic deposition [37,39,40]. The deposits will also reduce significantly the volume of electrolyte close to the surface and, thereby, will increase concentration gradients during current flow. Studies of polymer cells have linked the appearance of large concentration gradients close to the surface to the onset of dendritic deposition [36,41,42].

The images acquired for the conventional electrolyte system (Fig. 4) demonstrate the problems associated with operating a secondary battery with a lithium metal electrode. The finely divided deposit, which is likely to be a heterogeneous mass of metallic lithium and electrolyte reduction products, is an extremely reactive mass. The possibility that the heat generated by a short-circuit could ignite the deposit (and, hence, the remainder of the battery) in the presence of a volatile electrolyte renders the battery impractical for commercial use. In addition, the evident loss of capacity with

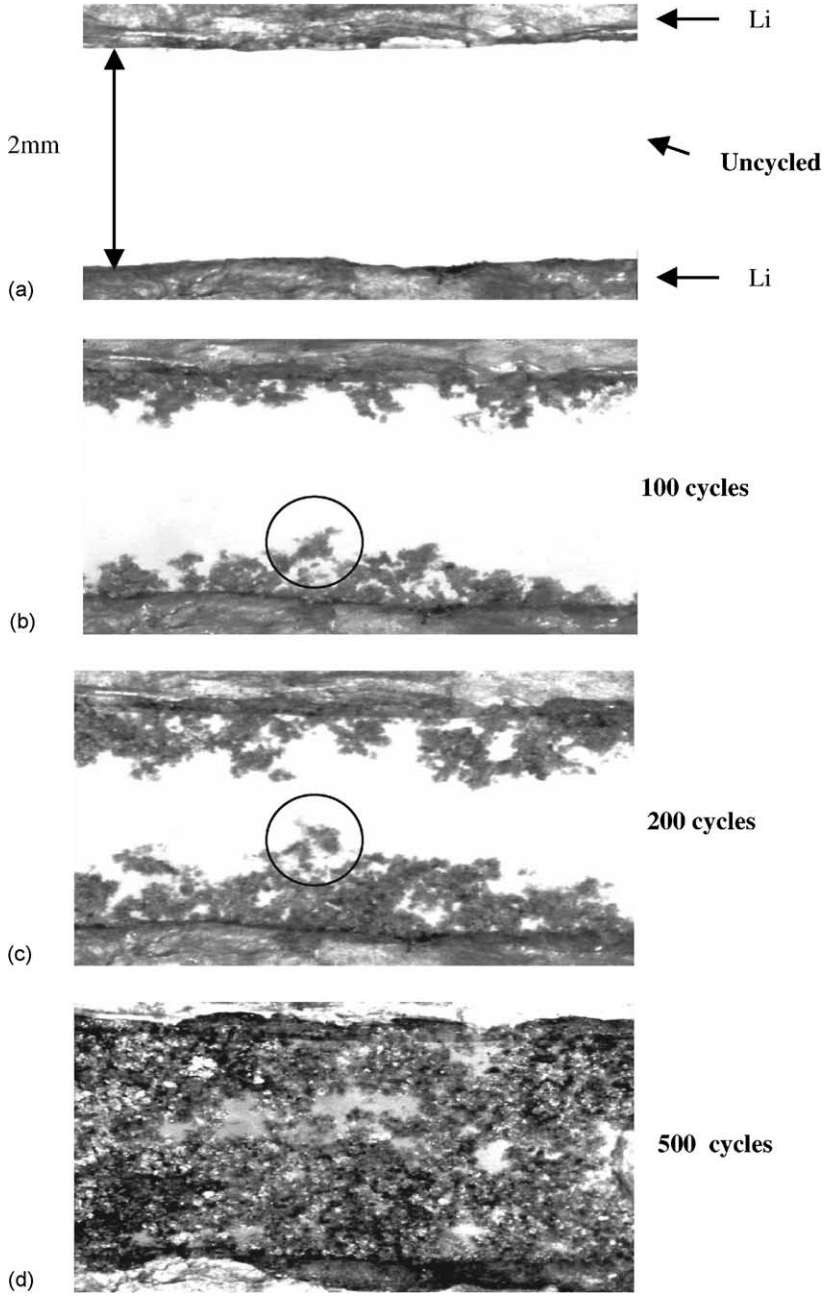

Fig. 4. Morphological changes during cycling of 1 M $LiPF_6$–PC cell at 1 mA cm^{-2}/1 C cm^{-2}.

cycling indicates a short life cycle for a battery that does not contain a large excess of lithium metal.

The incorporation of a borosilicate cover-slip into the cell design allows the in situ acquisition of Raman spectra of good quality, as shown in Fig. 6 for a PC–$LiPF_6$ cell after cycling. The upper and lower traces were obtained by focusing the beam in the bulk electrolyte at electrode depth and on the surface of a deposit formed during cycling, respectively. Both traces show peaks which arise from solvent vibrational modes. The surface trace displays additional modes which are thought to be due to the presence of species on the surface of the deposit. If this is the case, the most probable explanation for the detection of such small amounts of sample is due to a surface-enhanced resonance (SERS—Surface-Enhanced Raman Spectroscopy). Zeman and Schatz [43] have reported that the lithium surface can produce a Raman-enhanced signal. Thus, a Raman-enhancing substrate such as silver or gold, as has been used in most Raman studies of the lithium surface [44–47], may not be necessary in order to obtain SERS of lithium deposits. We have not yet been able to confidently assign vibrational modes to the additional peaks observed in the spectra shown in Fig. 6. It is considered that the acquisition of in situ Raman spectra will enable tracking of compositional

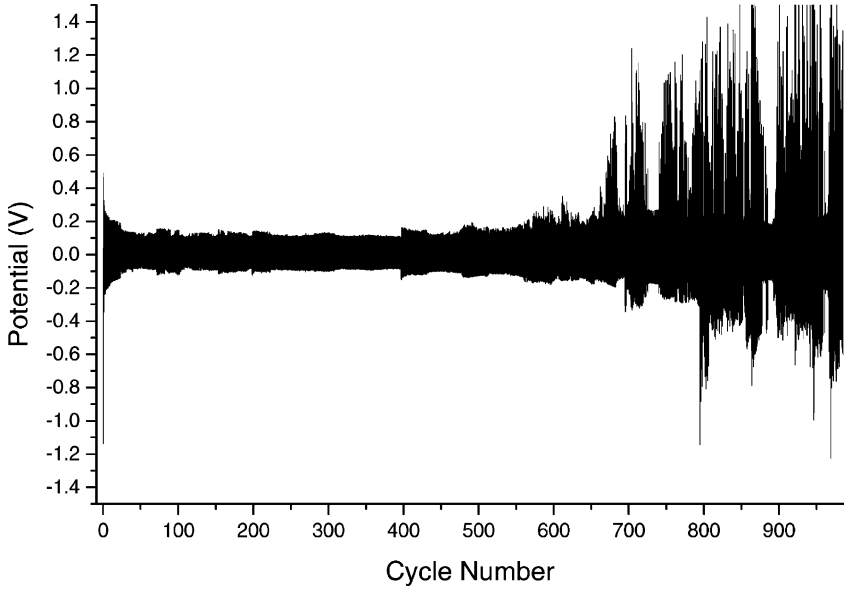

Fig. 5. Voltage profile for 1 M $LiPF_6$–PC cell under galvanostatic cycling.

changes in the electrolyte during charge–discharge cycling and identification of the surface deposits which are formed. Several studies of lithium–polymer cells have used Raman spectroscopy to measure concentration gradients at electrodes during current flow [42,48–50], and similar measurements may also be possible for liquid electrolytes using the optical cell developed in this study.

3.2. EMImTFSA–LiTFSA

Images obtained from a cell with EMImTFSA–LiTFSA electrolyte are presented in Fig. 7. The shaded area in the lower-left hand region of both images is a precipitate which appeared when attempting to cycle the cell at ambient temperature. The cell was then operated under similar conditions to the PC–$LiPF_6$ cell (Section 2.3), except that heating to 70 °C was necessary to overcome the large impedance at the interface. The appearance of the deposit remained unchanged when the cell was heated or subjected to cycling. It is apparent from the images that very different deposition morphology arises on the lithium surface in the ionic liquid. The combination of a compact interfacial layer and the attractive properties of the ionic liquid indicate that continued investigation of these materials for use as lithium battery electrolytes is warranted. The optical cell will be used in further studies to identify and evaluate ionic liquids which show promise as improved solvents for lithium rechargeable batteries.

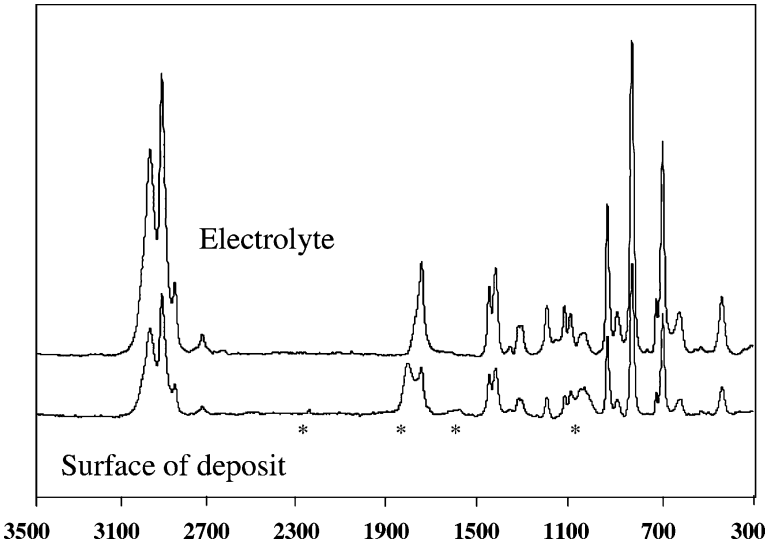

Fig. 6. In situ Raman spectra for 1 M $LiPF_6$–PC cell. Asterisks indicate additional modes associated with deposit surface.

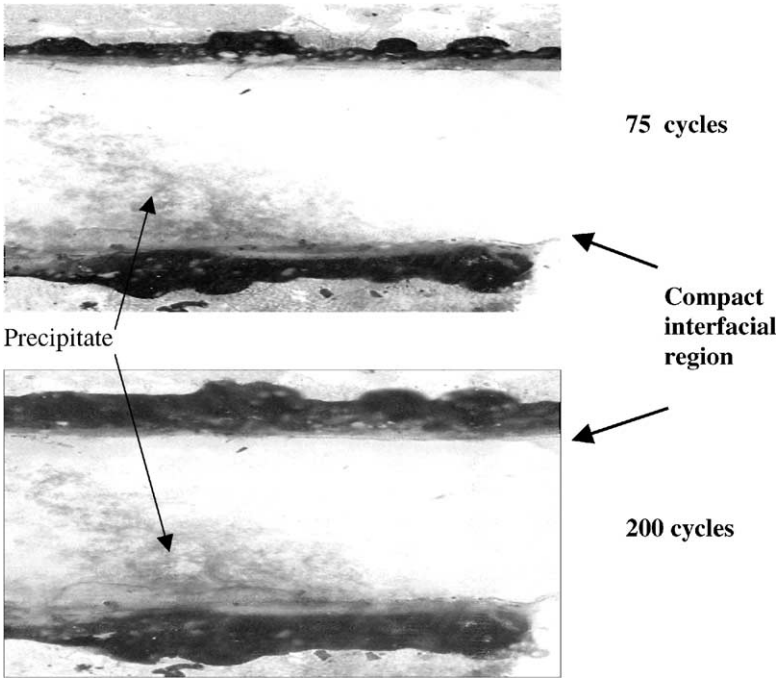

Fig. 7. Cycling of 20 mol% EMImTFSA–LiTFSA cell at 1 mA cm^{-2}/1 C cm^{-2}.

References

[1] E. Peled, J. Electrochem. Soc. 126 (1979) 2047.
[2] J.-I. Yamaki, S.I. Tobishima, in: J.O. Besenhard (Ed.), Handbook of Battery Materials, Wiley–VCH, Weinheim, Germany, 1999, p. 339.
[3] M. Odziemkowski, M. Krell, D.E. Irish, J. Electrochem. Soc. 139 (1992) 3052.
[4] K. Morigaki, A. Ohta, J. Power Sources 76 (1998) 159.
[5] K. Kanamura, H. Tamura, Z. Takehara, J. Electroanal. Chem. 333 (1992) 127.
[6] D. Aurbach, I. Weissman, H. Yamin, E. Elster, J. Electrochem. Soc. 145 (1998) 1421.
[7] K. Kanamura, H. Tamura, S. Shiraishi, Z.I. Takehara, Electrochim. Acta 40 (1995) 913.
[8] D. Aurbach, J. Electrochem. Soc. 136 (1989) 1606.
[9] D. Aurbach, J. Electrochem. Soc. 136 (1989) 1611.
[10] D. Aurbach, J. Power Sources 89 (2000) 206.
[11] D. Aurbach, M.L. Daroux, P.W. Faguy, E. Yeager, J. Electrochem. Soc. 134 (1987) 1611.
[12] D.P. Wilkinson, D. Wainwright, J. Electroanal. Chem. 355 (1993) 193.
[13] M.C. Borghini, M. Mastragostino, A. Zanelli, J. Power Sources 68 (1997) 52.
[14] Z. Jiang, B. Carroll, K.M. Abraham, Electrochim. Acta 42 (1997) 2667.
[15] G.B. Appetecchi, G. Dautzenberg, B. Scrosati, J. Electrochem. Soc. 143 (1996) 6.
[16] G.L.M.K.S. Kahanda, M. Tomkiewicz, J. Electrochem. Soc. 136 (1989) 1497.
[17] M. Arakawa, S. Tobishima, Y. Nemoto, M. Ichimura, J. Yamaki, J. Power Source 43 (1993) 27.
[18] M. Rosso, J.N. Chazalviel, V. Fleury, E. Chassaing, Electrochim. Acta 39 (1994) 507.
[19] J. Fuller, R.T. Carlin, R.A. Osteryoung, J. Electrochem. Soc. 143 (1996) L145–L147.
[20] C. Brissot, M. Rosso, J.N. Chazalviel, P. Baudry, S. Lascaud, Electrochim. Acta 43 (1998) 1569.
[21] I. Rey, J.L. Bruneel, J. Grondin, L. Servant, J.C. Lassegues, J. Electrochem. Soc. 145 (1998) 3034.
[22] J. Yamaki, S. Tobishima, K. Hayashi, S. Keiichi, Y. Nemoto, M. Arakawa, J. Power Sources 74 (1998) 219.
[23] C. Brissot, M. Rosso, J.N. Chazalviel, S. Lascaud, J. Power Sources 81 (1999) 925.
[24] T. Tatsuma, M. Taguchi, M. Iwaku, T. Sotomura, N. Oyama, J. Electroanal. Chem. 472 (1999) 142.
[25] C. Brissot, M. Rosso, J.N. Chazalviel, S. Lascaud, J. Power Sources 94 (2001) 212.
[26] T. Tatsuma, M. Taguchi, N. Oyama, Electrochim. Acta 46 (2001) 1201.
[27] K.R. Seddon, J. Chem. Technol. Biotechnol. 68 (1997) 351.
[28] J.D. Holbrey, K.R. Seddon, Clean Prod. Processes 1 (1999) 0223.
[29] S. Forsyth, J. Golding, D.R. MacFarlane, M. Forsyth, Electrochim. Acta 46 (2001) 1753.
[30] H. Ohno, Electrochim. Acta 46 (2001) 1407.
[31] J. Caja, T.D.J. Dunstan, V. Katovic, D.M. Ryan, in: Proceedings of the 39th Power Sources Conference, 12–15 June 2000, Cherry Hill, New Jersey, p. 124.
[32] J. Caja, T. Don, J. Dunstan, D.M. Ryan, V. Katovic, Molten Salts XII, vol. 99, Electrochemical Society Series, Electrochemical Society Inc., Pennington, New Jersey, p. 150.
[33] V.R. Koch, C. Nanjundiah, G.B. Appetecchi, B. Scrosati, J. Electrochem. Soc. 142 (1995) L116–L118.
[34] D.R. Macfarlane, J.H. Huang, M. Forsyth, Nature 402 (1999) 792.
[35] P. Bonhote, A.P. Dias, N. Papageorgiou, M. Armand, K. Kalyanasundaram, M. Gratzel, Inorg. Chem. 35 (1996) 1168.
[36] C. Brissot, M. Rosso, J.-N. Chazalviel, S. Lascaud, J. Power Sources 81 (1999) 925.
[37] J. Yamaki, S. Tobishima, K. Hayashi, S. Keiichi, Y. Nemoto, M. Arakawa, J. Power Sources 74 (1998) 219.
[38] C. Brissot, M. Rosso, J.-N. Chazalviel, P. Baudry, S. Lascaud, Electrochim. Acta 43 (1998) 1569.
[39] M. Arakawa, S. Tobishima, Y. Nemoto, M. Ichimura, J. Yamaki, J. Power Sources 43 (1993) 27.

[40] I. Yoshimatsu, T. Hirai, J. Yamaki, J. Electrochem. Soc. 135 (1988) 2422.
[41] M. Rosso, T. Gobron, C. Brissot, J.-N. Chazalviel, S. Lascaud, J. Power Sources 97–98 (2001) 804.
[42] C. Brissot, M. Rosso, J.-N. Chazalviel, S. Lascaud, J. Power Sources 94 (2001) 212.
[43] E.J. Zeman, G.C. Schatz, J. Phys. Chem. 91 (1987) 634.
[44] M. Odziemkowski, M. Krell, D.E. Irish, J. Electrochem. Soc. 139 (1992) 3052.
[45] H. Li, Y. Mo, N. Pei, X. Xu, X. Huang, L. Chen, J. Phys. Chem. B 104 (2000) 8477.
[46] H. Li, G. Li, Y. Mo, X. Huang, L. Chen, in: B.V.R. Chowdari, W. Wang (Eds.), Proceedings of the 7th Asian Conference, Solid State Ionics, World Scientific, Singapore, 2000.
[47] G. Li, H. Li, Y. Mo, L. Chen, X. Huang, J. Power Sources 104 (2002) 190.
[48] I. Rey, J.C. Lassègues, P. Baudry, H. Majastre, Electrochim. Acta 43 (1998) 1539.
[49] I. Rey, J.L. Bruneel, J. Grondin, L. Servant, J.C. Lassegues, J. Electrochem. Soc. 145 (1998) 3034.
[50] A. Ferry, M.M. Doeff, L.C. DeJonghe, Electrochim. Acta 43 (1998) 1387.